Proceedings of the 21st ICSMGE, Vienna, Austria, 14 – 19 June 2026. Pistrol, Adam & Schweiger (eds.)
Published by: ÖGG, Austrian Society for Geomechanics, Salzburg, Austria, ISBN 978-3-9503898-4-5
https://doi.org/10.53243/ICSMGE2026-729

Geohydro-mechanical interactions in numerical stability analyses of geotechnical structures

Jan Machaček
Department of Geotechnics, Federal Waterways Engineering & Research Institute, Karlsruhe, Germany
Institute of Geotechnics, Technical University Darmstadt, Germany, jan.machacek@tu-darmstadt.de

Emmanuel Bourgeois
HDR, Université Gustave Eiffel, France

Solveig Winkelmann, Eugen Perau
Institute of Geotechnical Engineering, University Duisburg-Essen, Germany

Holger Heidkamp
SOFiSTiK AG, Nürnberg, Germany

J.-Martin Hohberg
Dept. of Underground Structures, IUB Engineering AG, Berne, Switzerland

Tim Pucker
Geotechnics, HafenCity University Hamburg, Germany

David Remaud
itech-soft, Saint-Maurice, France

Oliver Reul
Department of Geotechnical Engineering, University Kassel, Germany

Oliver Stelzer
Department of Geotechnics, Federal Waterways Engineering & Research Institute, Karlsruhe, Germany

Christoph Schmüdderich
Chair of Soil Mechanics, Foundation Engineering and Environmental Geotechnics, Ruhr-University Bochum, Germany

Herbert Walter
Consulting Engineer, Salzburg, Austria

ABSTRACT: The stability analysis of geotechnical structures in the presence of groundwater flow, particularly in partially saturated soils, presents significant challenges in engineering practice. This study investigates the geohydro-mechanical coupling effects in steady-state and transient flow conditions on the stability analysis by means of two extensively analysed examples: (1) Stability of a backfilled cantilever retaining wall, evaluated under varying assumptions of soil type (sandy soil and silt) and groundwater boundary conditions. (2) Stability of an embankment composed of silt subjected to slow and rapid drawdown scenarios. Various modelling strategies are compared, with the focus on the impact of computational methods implemented across several software packages. Particular attention is given to partial saturation modelling, which significantly influences stability predictions. This study presents findings from the subgroup “Geohydro-Mechanical Interaction” of the working group "Numerical Methods in Geotechnical Engineering" (AK 1.6) of the German Geotechnical Society (DGGT). It builds on the working group’s 2014 recommendations (EANG) and extends a 2019 benchmark on stability analyses to include seepage. Based on these findings, practical recommendations are provided to assess the safety of geotechnical structures in the presence of groundwater.

KEYWORDS: groundwater flow, unsaturated soils, overall stability, geohydro-mechanical coupling, computational modelling

1 INTRODUCTION

The assessment of overall stability of geotechnical structures as a central task in geotechnical engineering is often governed by hydro-mechanical interactions, making their analysis more complex. Groundwater flow alters pore water pressure distributions, which directly affects the effective stress state and the available shear strength of the soil. While traditional limit-equilibrium methods have well-known limitations in complex scenarios, the Finite Element Method (FEM) has become a standard tool for analysing these coupled problems. The theoretical framework for these analyses is well-established, building on the effective stress principle and theories for unsaturated soil mechanics.

Despite the mature theoretical basis, a primary source of uncertainty in engineering practice arises from the variability in how different software packages implement the governing principles, particularly for unsaturated soils. This is especially true for the formulation of Bishop's effective stress parameter, χ, which controls the strength contribution from matric suction. This lack of uniformity complicates the application of design

standards such as Eurocode 7 (CEN, 2014), which provides specific guidance on stability calculations. The result is a potential for inconsistent and non-comparable stability predictions, even when identical input parameters are used. This need for clarity and consistency is a principal motivation for the present work.

To address these challenges and quantify the discrepancies, the subgroup "Geohydro-Mechanical Interaction" of the working group "Numerical Methods in Geotechnical Engineering" (AK 1.6) of the German Geotechnical Society (DGGT) initiated a comprehensive benchmark study. This paper presents the findings of this study, focusing on two distinct examples: a retaining wall under steady-state seepage and a reservoir embankment subjected to transient drawdown. By comparing results from multiple software packages and modelling strategies, the study evaluates the practical implications of different effective stress formulations, with a particular focus on the modelling of partial saturation. The aim is to provide practical recommendations for engineers to ensure the reliable and standard-compliant stability assessment of geotechnical structures under the influence of groundwater.

2 GOVERNING PRINCIPLES

2.1 *Saturated conditions*

In fully saturated soils, the mechanical response is governed by the effective stress principle formulated by Terzaghi and Fröhlich (1936). The effective stress, $\boldsymbol{\sigma}'$, is defined as the difference between the total stress, $\boldsymbol{\sigma}$, and the pore water pressure, p^w. The fluid flux is usually described by Darcy's law, which relates the volumetric flow rate of water to the hydraulic gradient and the soil's saturated hydraulic conductivity. Combined, these governing equations define the evolution of pore pressure fields, which directly influence effective stresses and thereby control the deformation and stability of geotechnical systems.

2.2 *Unsaturated conditions*

In unsaturated soils, both the hydraulic and mechanical governing relations must be extended for more realistic simulations. The interested reader is referred to literature such as Fredlund et al. (2012) and Lu (2020) for a comprehensive overview.

2.2.1 *Hydraulic behaviour*

The hydraulic behaviour of an unsaturated soil is characterized by the soil-water retention curve (SWRC), which describes the highly nonlinear relationship between suction (s) and the degree of saturation (S^w). The van Genuchten (1980) model is widely used to represent the SWRC. A critical aspect of unsaturated flow is the significant reduction in hydraulic conductivity for $S^w < 1$. The unsaturated hydraulic conductivity, K, is typically expressed as the product of the saturated hydraulic conductivity, K^{sat}, and a relative permeability function, k^{rel}, which depends on the degree of saturation. When combined with the van Genuchten SWRC, the Mualem (1976) model is commonly used to define this relationship:

$$K = k^{rel}K^{sat} = \sqrt{S^e}\left[1 - \left(1 - (S^e)^{1/m}\right)^m\right]^2 K^{sat} \qquad (1)$$

where $S^e = (S^w - S^{res})/(1 - S^{res})$ is the effective degree of saturation and m is a parameter related to the pore-size distribution, often set as $m = 1 - 1/n_{vG}$ from the van Genuchten shape parameter n_{vG}. S^{res} is the residual degree of saturation. The same formulation is incorporated in all software packages used in this work; thus, no further elaboration is needed.

2.2.2 *Mechanical behaviour and effective stress*

For unsaturated conditions, the effective stress concept must be generalized to account for the effect of suction (s). Bishop (1959) proposed an extended formulation for the effective stress tensor:

$$\boldsymbol{\sigma}' = \boldsymbol{\sigma} + \chi s\boldsymbol{\delta} \qquad (2)$$

where $\boldsymbol{\sigma}$ is the total stress, χ is a material-dependent weighting function that modulates the contribution of suction to the effective stress and $\boldsymbol{\delta}$ is the Kronecker-Delta. The primary challenge lies in the definition of χ. Various formulations are available and implemented across different software packages, resulting in a significant impact of the user's selection on the outcome of stability calculations. The most common formulations in engineering practice are two definitions:

$$\chi = S^w \quad \text{or} \quad \chi = S^e. \qquad (3)$$

When used in combination with a linear elastic constitutive model with Mohr-Coulomb failure criterion, the influence of these formulations on the shear strength can be quantified through an apparent cohesion (c^{app}), which acts as an additional component to the soil's effective cohesion. This is given by the relation:

$$c^{\text{app}} = \chi s \tan\varphi', \qquad (4)$$

While simple to implement, these linear models for χ have known deficiencies such as the prediction of unrealistically high shear strengths at low saturation levels. As illustrated in Figure 1 for the parameters of a typical silt given in Table 2, the assumption of $\chi = S^w$ leads to an unbounded increase in apparent cohesion, reaching unphysical values at suction levels above 100 kPa.

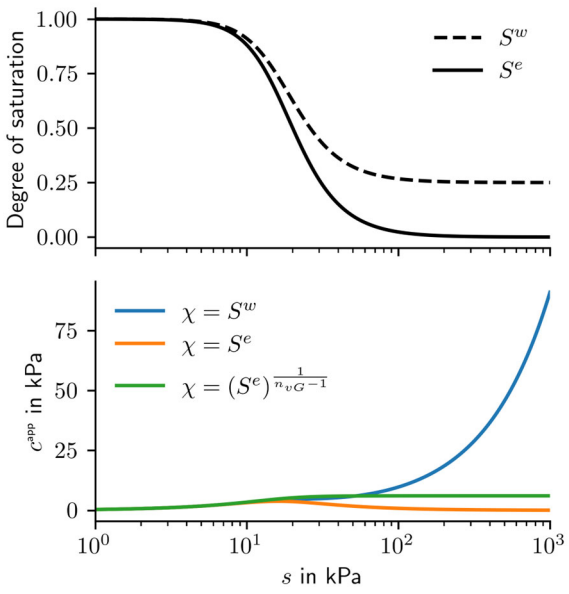

Figure 1. Comparison of apparent cohesion (bottom) derived from different effective stress models, based on the soil-water retention curve for silt shown (top).

To address this, alternative formulations have been proposed, such as the power-law formulation implemented in ZSoil (Truty, 2023), which establishes a link between the mechanical parameter χ and the hydraulic properties of the soil via the van Genuchten shape parameter n_{vG} and limits the contribution of suction to the effective stress even at high suction values.

$$\chi = (S^e)^{\alpha} \quad \text{where} \quad \alpha = \frac{1}{n_{vG} - 1} \qquad (5)$$

2.3 *Implications for numerical stability analysis*

In engineering design, it is common practice and consistent with Eurocode 7 to conservatively neglect any strength contribution from suction ($\chi = 0$). However, the formulation of effective stress varies across finite element codes, and not every software allows the user to easily deactivate the contribution of suction to the effective stress. This discrepancy may induce unintentional and non-conservative strength enhancement to the analysis.

The conflict between a conservative design approach and software implementation complicates transparent benchmarking and can lead to designs that are not in compliance with EC 7. It is therefore imperative that practitioners understand the specific effective stress model implemented in their chosen software to correctly interpret stability results.

To investigate the practical impact of the software-specific implementations discussed above, two benchmark tests were conducted. The software packages used by the different working groups are detailed in Table 1, which specifies the available effective stress formulations for each program - the central issue highlighted in the previous section.

Most analyses were performed using the Finite Element Method (FEM) with a strength reduction approach. For comparison, calculations were also carried out using a classical limit equilibrium analysis (LEA) according to DIN 4084, specifically Janbu's (retaining wall benchmark) and Bishop's (embankment benchmark) method of slices (via the GGU software package). Note that LEA does not allow for fully coupled calculations and, by default, neglects suction stresses, providing a distinct contrast to the coupled FEM analyses.

Table 1. Software packages used in the benchmark study and their available effective stress formulations

		$\chi =$			
Software	Version	0	S^w	S^e	$(S^e)^\alpha$
CESAR	2025.0	✓			
numgeo	2024-12	✓		✓	✓
Optum G2	2020v2.0	✓		✓	
PLAXIS 2D	2024.2	✓		✓	
Rocscience-RS2	11			✓	
SOFiSTiK	2024-4	✓	(✓)		
ZSoil	24.06		✓		✓
GGU-Stability	V14	✓			
GGU-2D-SSFlow +	V11				
GGU-2D-Transient	V7				

3 RETAINING WALL – STEADY-STATE GROUNDWATER FLOW

The first benchmark investigates the stability of an cantilever retaining wall, a system based on a previously published computational example (Perau and Schneider, 2009; Wolffersdorff, 2019). The primary objective is to quantify the influence of a rising groundwater table and the consequent steady-state seepage on the structure's factor of safety. The analysis is performed for two different backfill materials, silt and sand, to assess the role of soil type in the hydro-mechanical response.

3.1 *Model definition and numerical analysis*

The model geometry, depicted in Figure 2, consists of a backfilled cantilever retaining wall with an embedment depth of 2 m. The wall, founded on a 0.5 m-thick sand layer, is modelled as a linear elastic material with a unit weight of 25 kN/m³, a Young's modulus of 40 GPa and a Poisson's ratio of 0.2. The analysis was conducted for two different homogeneous soil profiles: one consisting entirely of silt and the other of sand. In the numerical analyses, both soil profiles were described using a linear elastic-perfectly plastic model with a Mohr-Coulomb failure criterion. The corresponding material parameters are provided in Table 2.

The initial porosity was set to 0.4 and the initial ground water level was located at an elevation of -2.5 m. To simulate the effect of a rising groundwater (gw) table, steady-state hydraulic boundary conditions were applied. The gw potential was fixed at the ground surface (elevation ±0.0 m) along the left-hand boundary and was incrementally raised from -2.5 m to +6.0 m at the right-hand boundary. The base of the model was treated as an impervious boundary.

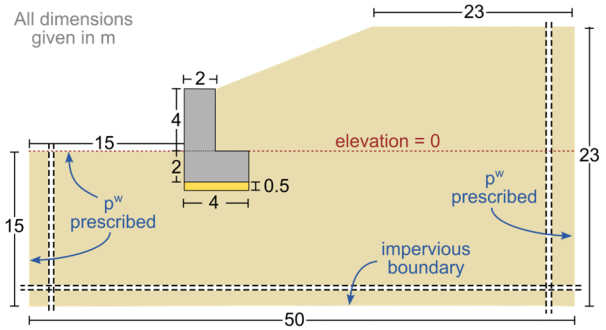

Figure 2. Retaining wall benchmark: Geometry and hydraulic boundary conditions

Table 2. Retaining wall benchmark: Material and interface parameters

Parameter			Silt	Sand
Unit weight	γ	(kN/m³)	20	20
Sat. unit weight	γ^{sat}	(kN/m³)	20	20
Young's modulus	E	(MN/m²)	40	40
Poisson's ratio	ν	(-)	0.3	0.3
Cohesion	c	(kN/m²)	10	0.1
Friction angle	φ'	(°)	20	35
Dilatancy angle	ψ	(°)	0	5
Interface friction angle	δ	(°)	13.33	23.33
Interface adhesion	a	(kN/m²)	0.1	0.1
Sat. hyd. conductivity	K^{sat}	(m/s)	10^{-6}	10^{-4}
Residual saturation	S^{res}	(-)	0.25	0.086
Van Genuchten parameter	α_{vG}	(1/m)	0.6	3.2
	n_{vG}	(-)	3.1	3.1
	m	(-)	0.68	0.68

The simulations were performed as uncoupled analyses, where each incremental rise in groundwater was considered as separate steady-state flow problem. The analysis sequence replicated the construction history, followed by the step-wise increase of the water table as detailed in Walter et al. (2025). After each step, a strength reduction analysis was conducted to determine the factor of safety (FoS).

The software packages used varied in their element types (stabilized first-order rectangular, second-order and fourth-order triangular elements) and mesh discretization, ranging from approximately 15,000 to 30,000 nodes (Walter et al., 2025).

3.2 *Results and discussion*

This section presents the results of the benchmark analyses, with a focus on both the hydraulic and mechanical responses of the system.

The steady-state hydraulic analyses show a high level of agreement among the different software packages. The computed pore water pressure distributions and the location of the phreatic surface differ only marginally. Figure 3 illustrates the calculated phreatic surfaces for the case of the silt, highlighting the consistency across codes despite differences in discretisation and numerical formulation.

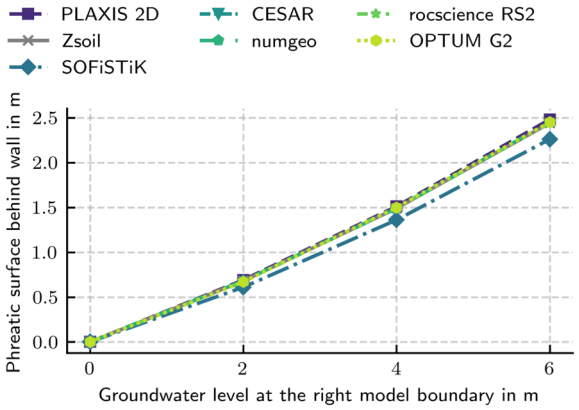

Figure 3. Retaining wall; silt: Comparison of the phreatic surface location

In all simulations, the stability analyses identify a global failure mechanism involving sliding of the backfill and rotation with head deflection of the retaining wall. Figure 4 displays the failure mechanism for the silt profile in terms of incremental deviatoric strains computed by PLAXIS 2D. Figure 5 summarises the factor of safety (FoS) values for the silt profile as a function of groundwater elevation on the right-hand boundary. With increasing water level, all programs predict a monotonic reduction in the FoS, which is consistent with theoretical expectations.

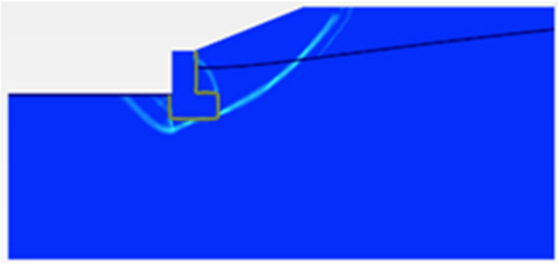

Figure 4. Retaining wall; silt; gw level = +6.0 m: Predicted failure mechanism illustrated by incremental deviatoric strains at failure as calculated with PLAXIS 2D

Despite the close agreement in the hydraulic results, the calculated FoS values vary significantly across software packages. These discrepancies are not attributable to differences in pore pressure fields but are more plausibly explained by variations in the mechanical treatment of suction.

As illustrated in Figure 1, the choice of weighting function χ has a direct impact on the shear strength under unsaturated conditions. Eurocode 7 explicitly recommends that the contribution of suction to shear strength be neglected in ultimate limit state design to ensure a conservative design approach. However, as shown in Table 1, only a subset of the employed software packages provides the option to set $\chi = 0$ and to fully deactivate suction effects. An alternative approach involves defining a steep soil-water retention curve (SWRC) to minimise the extent of the capillary fringe. While this may reduce suction-induced increases in shear strength, it also alters the relative permeability and flow behaviour. For this reason, such results are excluded from further analysis.

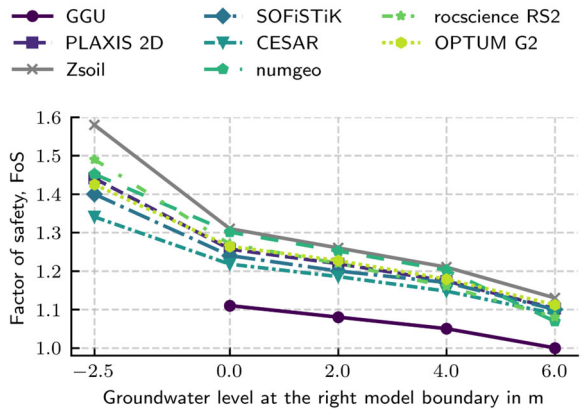

Figure 5. Retaining wall; silt: FoS as a function of groundwater level (suction effects included)

To quantify the influence of the effective stress model on predicted stability, a comparative analysis is conducted for four different χ formulations. Figure 6 presents the FoS results for silt and sand, grouped by the selected effective stress model. The shaded areas indicate the standard deviation of results among the contributing software packages.

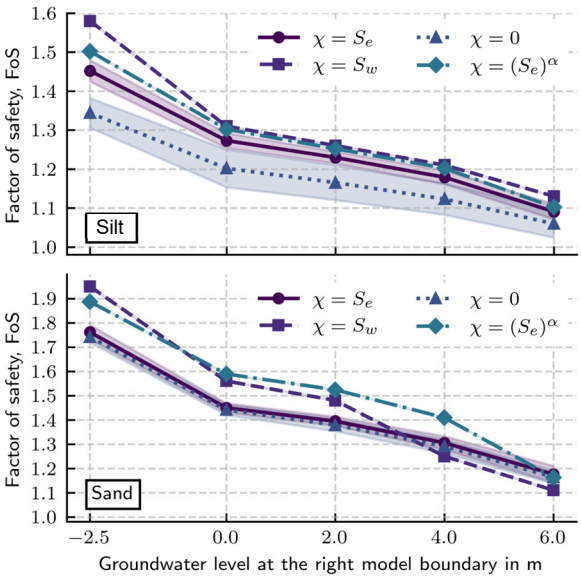

Figure 6. Retaining wall: Influence of effective stress (χ) formulation on the predicted FoS. Shaded areas denote the standard deviation

The findings confirm that neglecting suction (i.e. $\chi = 0$) yields the lowest and most conservative safety factors. Conversely, adopting a linear or power-law weighting function results in higher FoS values, particularly at lower groundwater levels where matric suction is significant.

The results underline the importance of transparency in the implementation of suction effects in numerical models. Inconsistent or undocumented assumptions regarding χ may compromise the comparability of simulations and the reliability of stability assessments. Engineers must be aware of how their selected software handles unsaturated soil mechanics and must verify whether the implemented assumptions align with project-specific design requirements and standards - particularly for structures with narrow safety margins.

4 EMBANKMENT SUBJECTED TO RAPID AND SLOW DRAWDOWN

The second benchmark examines the stability of an embankment of a reservoir subjected to transient drawdown conditions, with a particular focus on the influence of drawdown rate on pore water pressure dissipation and slope stability.

4.1 *Model definition and numerical analysis*

The model geometry is depicted in Figure 7. The left boundary of the model represents an axis of symmetry, while the right boundary features an impervious internal core extending to the base of the model. Consequently, the left, right, and bottom model boundaries are all defined as impervious (no-flow) boundaries.

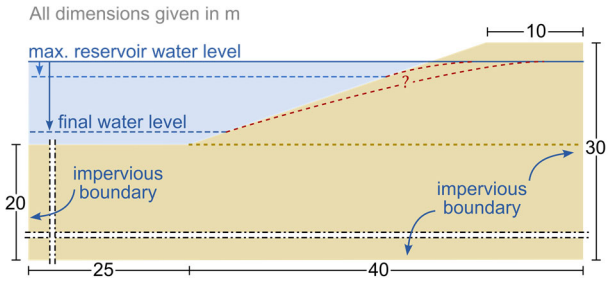

Figure 7. Embankment benchmark, geometry and hydraulic boundary conditions

The embankment and the subsoil consist of silt, which is described using a linear elastic-perfectly plastic model with a Mohr-Coulomb failure criterion. The shear strength parameters for the silt deviate slightly from the silt used in the first example and are defined with an effective friction angle (φ') of 27.5°, an effective cohesion (c') of 5 kN/m², a dilatancy angle (ψ) of 10° and a Young's modulus of 15 MN/m². All other material properties were identical to those specified for the silt in Table 2.

The numerical simulations were conducted using coupled hydro-mechanical analysis for the different FEM-based software packages. The initial state for the simulation is defined by a horizontal ground surface with a coincident groundwater level (GWL) at an elevation of +20.0 m from the model base, as depicted by the dashed brown line in Figure 7. From this initial state, the embankment construction is simulated. A steady-state seepage analysis is then performed to determine the hydraulic conditions corresponding to the reservoir's high-water level (HWL) of +29.0 m. Subsequently, a transient analysis was performed to simulate the drawdown of the reservoir over 8 m to the final water level of +21.0 m. Two distinct scenarios were investigated:

- Rapid drawdown: The drawdown occurs over 1 day.
- Slow drawdown: The drawdown occurs over 8 days.

After each drawdown interval of one meter, a strength reduction analysis was performed to determine the evolution of the FoS. For comparison, uncoupled LEA, which neglect suction stresses, were also conducted.

4.2 *Results and discussion*

The results of the transient analysis are discussed in two distinct phases: the stability of the embankment during the reservoir drawdown and its subsequent long-term stability recovery after the drawdown is complete.

4.2.1 *Stability during reservoir drawdown*

All numerical models predicted a consistent slope failure mechanism, with a failure surface geometry that was largely independent of the drawdown rate. The rate of drawdown, however, has a pronounced effect on the calculated FoS. The rapid drawdown scenario results in significantly lower FoS values at all stages compared to the slow drawdown scenario, as shown in Figure 8. This reduction in stability can be attributed to the larger excess pore water pressures and the development of destabilizing, outward-directed hydraulic gradients that occur during rapid drawdown due to delayed drainage in the low-permeability silt.

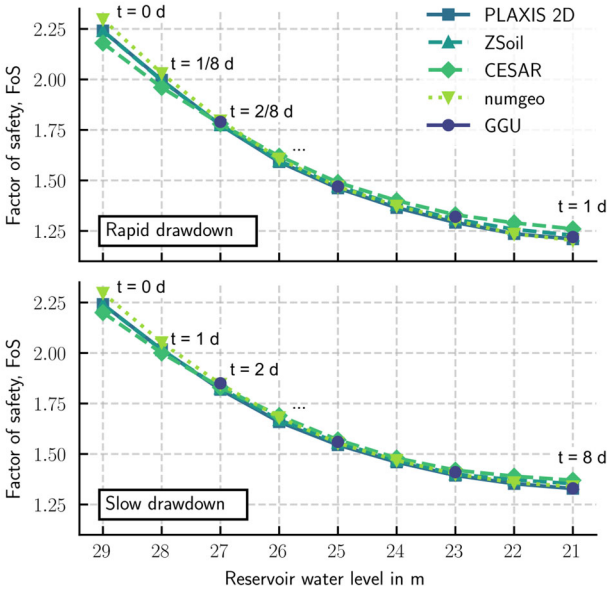

Figure 8. Embankment: FoS as a function of reservoir water level (suction effects included)

The influence of the effective stress formulation on the slope stability was also investigated. As illustrated for the slow drawdown case in Figure 9 analyses that neglect suction effects ($\chi = 0$) yield consistently lower and more conservative FoS values, which is aligned with theoretical expectations.

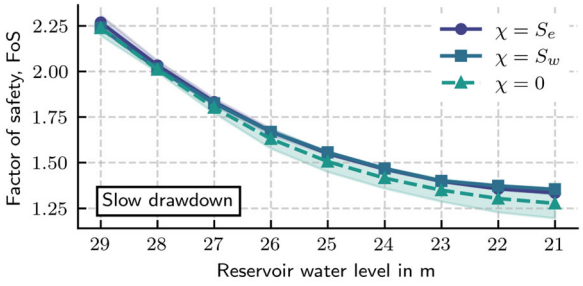

Figure 9. Embankment: Influence of different effective stress (χ) formulations on the FoS as a function of reservoir water level

4.2.2 *Stability during post-drawdown consolidation*

Following the completion of the drawdown to an elevation of +21 m above the model base, the long-term stability recovery was investigated by simulating additional consolidation stages with specific time intervals of 1, 10, 100, 1000, and 10,000 days. A strength-reduction analysis was conducted after each of these consolidation stages to determine the corresponding FoS.

The results show an increase of the FoS as consolidation progresses, eventually approaching a final steady state value. This development is illustrated in Figure 10, which plots the FoS as a function of time for the rapid drawdown scenario. This recovery in stability corresponds to the gradual lowering of the phreatic surface within the embankment as it drains towards its

final long-term equilibrium position (steady state), as depicted in Figure 11.

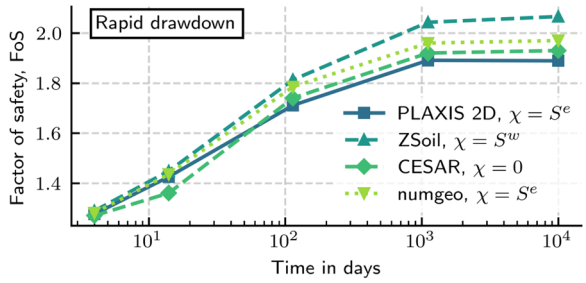

Figure 10. Embankment: Development of FoS during consolidation after lowering the reservoir water level to 21 m above model base.

A key finding from this analysis phase is that significant deviations emerge and increase between the software packages during the long-term consolidation even though results were in good agreement during the drawdown. These deviations are attributed to the different default effective stress (χ) models used by the software. Notably, the software packages employing $\chi = S^e$ as their default (PLAXIS 2D and numgeo) achieve the closest agreement for the final steady-state FoS. In contrast, ZSoil, which defaults to $\chi = S^w$, predicts a higher final FoS, a result that is consistent with the findings from Sections 2.2.2 and 3.2.

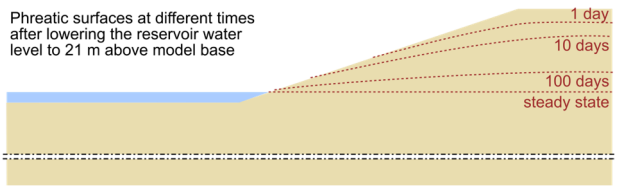

Figure 11. Embankment: Phreatic surfaces at different times as calculated with numgeo.

5 SUMMARY AND CONCLUSION

This benchmark study compared the performance of several finite element software packages in solving two distinct geohydro-mechanical overall stability problems. The evaluation indicates that while the participating codes can determine hydraulic phenomena with a high degree of consistency, particularly for steady-state conditions, this agreement does not extend to stability analyses.

The stability results exhibited considerable variance, especially in the first benchmark example, where the influence of partial saturation was most prominent. The primary source of this variance was identified as the different software-specific implementations of the effective stress principle for unsaturated soils, specifically the formulation of Bishop's effective stress variable, χ. The choice of this parameter is not a minor modeling detail but a decisive factor that can alter the outcome of stability verifications. As demonstrated, neglecting suction stresses ($\chi = 0$), as recommended by design standards such as Eurocode 7, not only provides the most conservative FoS but also demonstrably reduces the scatter among the results from different software packages.

Beyond the dominant effect of the effective stress model, other factors inherent to numerical implementation also contribute to the observed discrepancies. These include differences in global iterative solution schemes and their tolerance limits, the choice of element formulations and mesh discretization, and other constitutive assumptions related to non-associated plasticity or unit weight calculations.

This study highlights the imperative for engineers to be critically aware of the underlying theoretical assumptions – particularly concerning unsaturated soil mechanics – within their chosen computational tools. This awareness is essential for the correct interpretation of numerical results and the execution of standard-compliant designs, especially for structures with narrow safety margins. Future work by the group "Geohydro-Mechanical Interaction" will extend these benchmark activities to other important (geo)hydro-mechanical problems, such as excavation dewatering and rainfall-induced slope (in)stability.

6 ACKNOWLEDGEMENTS

The authors gratefully acknowledge Kristian and Jørgen Krabbenhøft (Optum Computational Engineering, Copenhagen, Denmark) for the calculations with Optum G2 and Sina Moallemi (Rocscience, Toronto, Canada) for the calculations with Rocscience RS2. The authors are grateful to all contributors for providing their computational results and for their valuable feedback during the preparation of this manuscript.

7 REFERENCES

Bishop, A.W., 1959. The principle of effective stress. *Teknisk Ukeblad*, 39, pp.859–863.

CEN, 2014. EN 1997-1:2014, Eurocode 7: Geotechnical design – part 1: General rules. Brussels: European Committee for Standardisation (CEN).

Fredlund, D.G., Rahardjo, H. and Fredlund, M.D., 2012. Unsaturated soil mechanics in engineering practice. Fredlund/Unsaturated Soil Mechanics. John Wiley & Sons, Inc. https://doi.org/10.1002/9781118280492.

van Genuchten, M.Th., 1980. A Closed-form Equation for Predicting the Hydraulic Conductivity of Unsaturated Soils. Soil Science Society of America Journal, 44(5), pp.892–898. https://doi.org/10.2136/sssaj1980.03615995004400050002x.

Lu, N., 2020. Unsaturated Soil Mechanics: Fundamental Challenges, Breakthroughs, and Opportunities. Journal of Geotechnical and Geoenvironmental Engineering, 146(5), p.02520001. https://doi.org/10.1061/(ASCE)GT.1943-5606.0002233.

Mualem, Y., 1976. A new model for predicting the hydraulic conductivity of unsaturated porous media. Water Resources Research, 12(3), pp.513–522. https://doi.org/10.1029/wr012i003p00513.

Perau, E. and Schneider, U., 2009. Nachweise zur Standsicherheit von Dammböschungen - ein Vergleich zwischen klassischen Verfahren und der FEM, Sicherung von Dämmen, Deichen und Stauanlagen. In: Handbuch für Theorie und Praxis. Universitätsverlag universi Siegen. pp.265–288.

Terzaghi, K. and Fröhlich, O.K., 1936. Theory of settlement of clay layers. Franz Deuticke.

Truty, A., 2023. New developments in ZSoil v2023 midyear upgrade. Why do we need full van Genuchten's law, Biot coefficient and modified Bishop effective stress principle ? [online] Available at: <https://zsoil.com/zsoil_day/2023/08-Truty-ZSoilDay2023-New_features_in_ZSoil_v23-50.pdf>.

Walter, H., Buscher, S., Heidkamp, H., Hohberg, M., Machaček, J., Perau, E., Pucker, T., Reul, O. and Stelzer, O., 2025. Berechnungen von Grundwasserströmungen mit der FEM und deren Auswirkung auf die Standsicherheit. In: Proceedings of the 39. Christian Veder Kolloquium (CVK). [online] 39. Christian Veder Kolloquium. Graz, Austria: Technische Universität Graz, Institut für Bodenmechanik, Grundbau und Numerische Geotechnik. pp.247–264. https://doi.org/10.3217/reqpc-9fg52.

Wolffersdorff, P., 2019. Informationen und Empfehlungen des Arbeitskreises 1.6 „Numerik in der Geotechnik": Berechnung der Standsicherheit mit der FEM durch Reduzierung der Festigkeitsparameter. geotechnik, 42(2), pp.88–97. https://doi.org/10.1002/gete.201900006.